

**Cell Reports, Volume 43**

**Supplemental information**

**Perisaccadic and attentional remapping  
of receptive fields in lateral  
intraparietal area and frontal eye fields**

**Xiao Wang, Cong Zhang, Lin Yang, Min Jin, Michael E. Goldberg, Mingsha  
Zhang, and Ning Qian**

## Supplementary Information

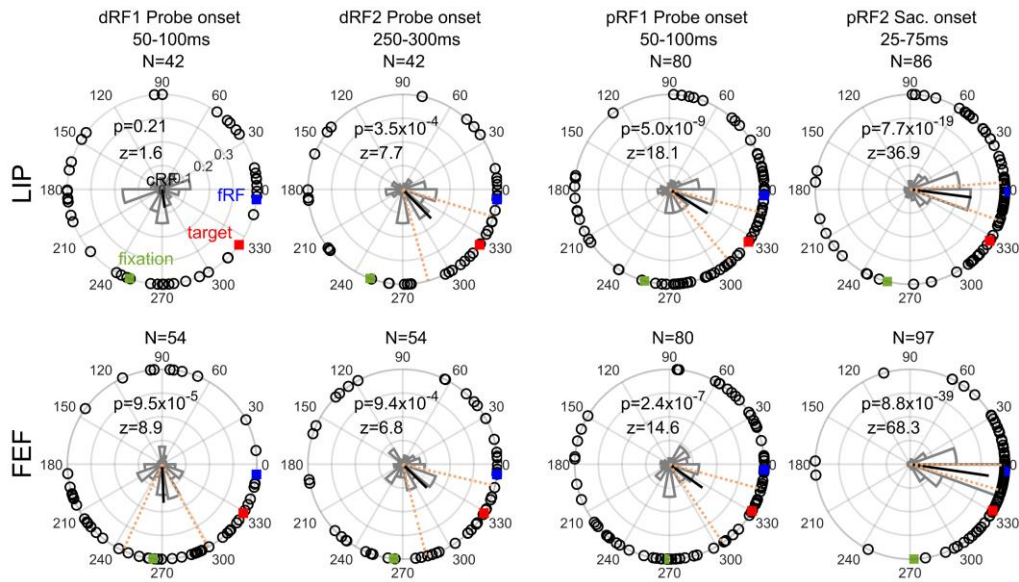


Fig. S1. RF remapping in LIP and FEF, related to Fig. 2b and StarMethods. The delay (dRF) and perrisaccadic (pRF) shift directions of LIP (top row) and FEF (bottom row) cells from different time periods (columns) are shown. The contour criterion was 85% and the completeness criterion was 90%. The format was identical to that of Fig. 2b of the main text. The mean directions changed significantly across time in both LIP ( $p = 2.5 \times 10^{-4}$ ,  $F_{3,246} = 6.6$ ) and FEF ( $p = 1.9 \times 10^{-9}$ ,  $F_{3,281} = 15.7$ ), with Watson-Williams multi-sample test.

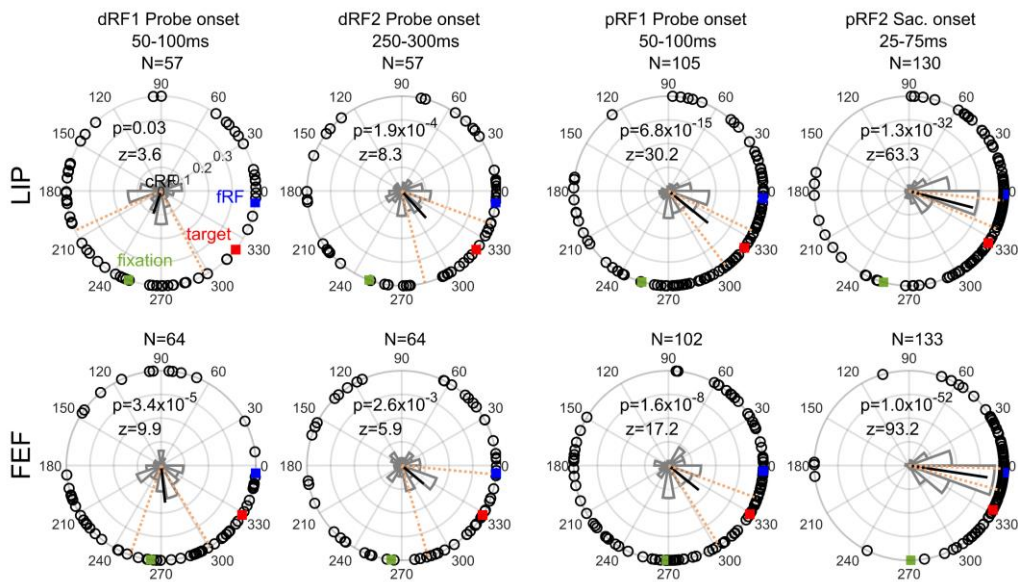


Fig. S2. RF remapping in LIP and FEF, related to Fig. 2b and StarMethods. The delay (dRF) and perrisaccadic (pRF) shift directions of LIP (top row) and FEF (bottom row) cells from different time periods (columns) are shown. The contour criterion was 85% and the completeness criterion was 70%. The format was identical to that of Fig. 2b in the main text. The mean directions changed significantly across time in both LIP ( $p = 3.6 \times 10^{-9}$ ,  $F_{3,345} = 14.9$ ) and FEF ( $p = 1.7 \times 10^{-10}$ ,  $F_{3,359} = 17.3$ ), with Watson-Williams multi-sample test.

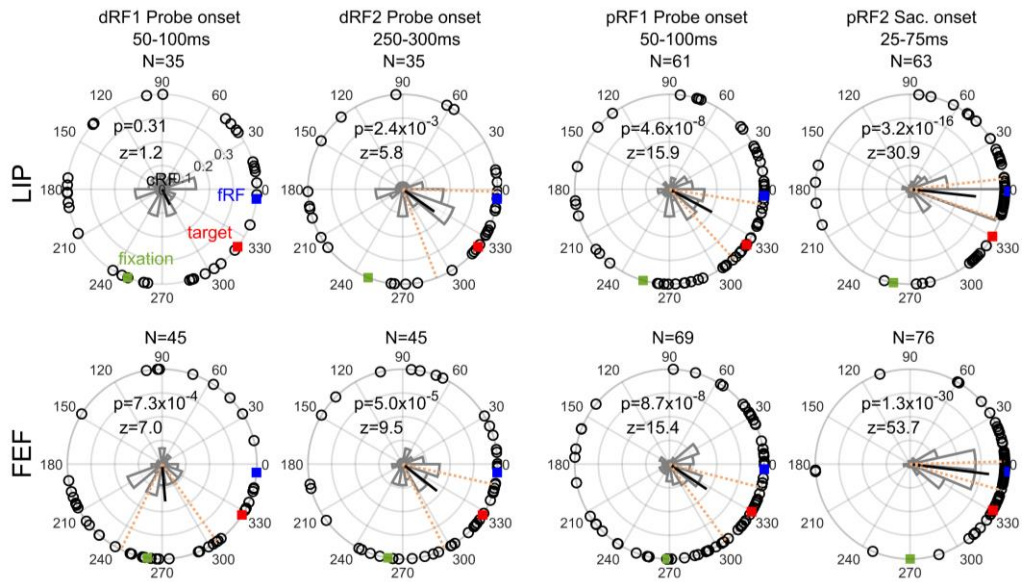


Fig. S3. RF remapping in LIP and FEF, related to Fig. 2b and StarMethods. The delay (dRF) and perrisaccadic (pRF) shift directions of LIP (top row) and FEF (bottom row) cells from different time periods (columns) are shown. The contour criterion was 75% and the completeness criterion was 90%. The format was identical to that of Fig. 2b in the main text. The mean directions changed significantly across time in both LIP ( $p = 0.021$ ,  $F_{3,190} = 3.3$ ) and FEF ( $p = 1.4 \times 10^{-7}$ ,  $F_{3,231} = 12.5$ ), with Watson-Williams multi-sample test.

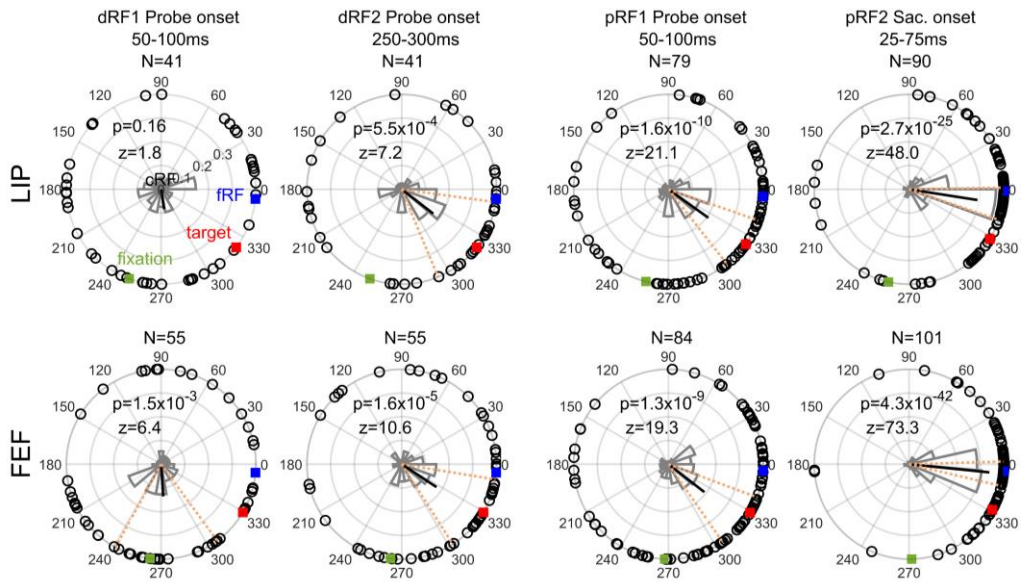


Fig. S4. RF remapping in LIP and FEF, related to Fig. 2b and StarMethods. The delay (dRF) and perrisaccadic (pRF) shift directions of LIP (top row) and FEF (bottom row) cells from different time periods (columns) are shown. The contour criterion was 75% and the completeness criterion was 80%. The format was identical to that of Fig. 2b in the main text. The mean directions changed significantly across time in both LIP ( $p = 1.9 \times 10^{-4}$ ,  $F_{3,247} = 6.8$ ) and FEF ( $p = 2.5 \times 10^{-9}$ ,  $F_{3,291} = 15.4$ ), with Watson-Williams multi-sample test.

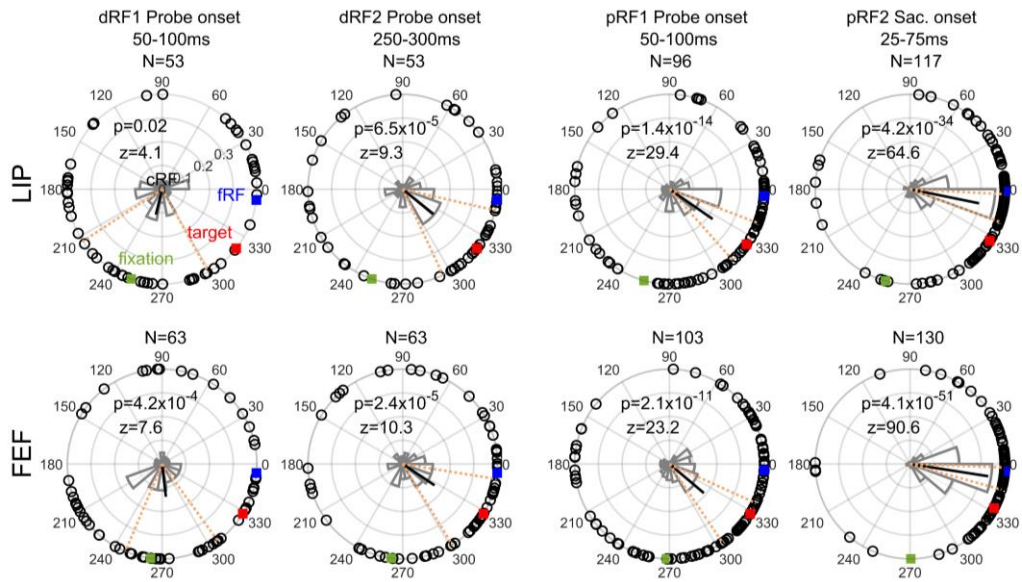


Fig. S5. RF remapping in LIP and FEF, related to Fig. 2b and StarMethods. The delay (dRF) and perrisaccadic (pRF) shift directions of LIP (top row) and FEF (bottom row) cells from different time periods (columns) are shown. The contour criterion was 75% and the completeness criterion was 70%. The format was identical to that of Fig. 2b in the main text. The mean directions changed significantly across time in both LIP ( $p = 6.7 \times 10^{-9}$ ,  $F_{3,315} = 14.5$ ) and FEF ( $p = 7.0 \times 10^{-10}$ ,  $F_{3,355} = 16.2$ ), with Watson-Williams multi-sample test.

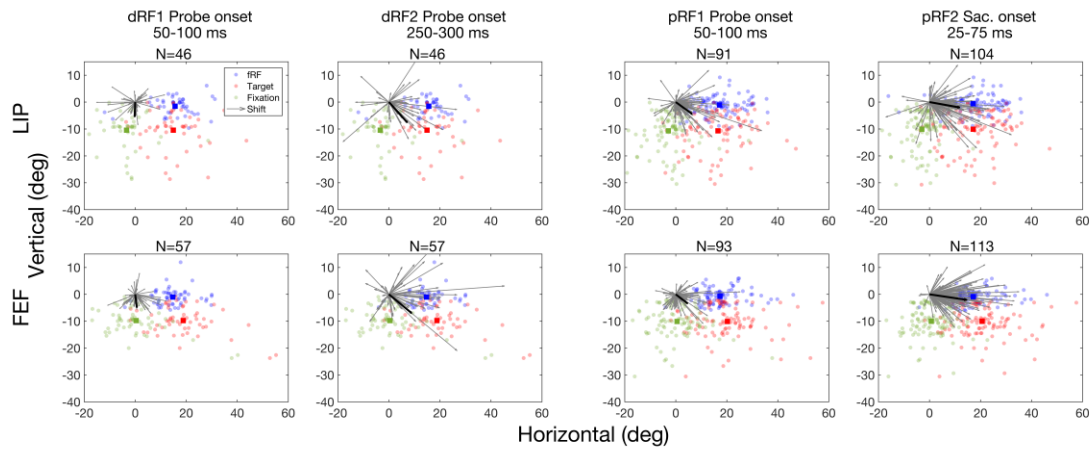


Fig. S6. RF remapping in LIP and FEF, related to Fig. 2b and StarMethods. The delay (dRF) and perrisaccadic (pRF) shift vectors of LIP (top row) and FEF (bottom row) cells from different time periods (columns) are shown. This figure corresponds to Fig. 2b of the main text but shows both the shift direction and amplitude of each cell. In each panel, we align the cells' cRF centers at (0, 0) and saccade directions along positive horizontal. The cells' fRF centers, the targets, and the initial-fixation points are shown as blue, red, and green dots, respectively, and their mean positions as the blue, red, and green squares, respectively. Gray arrows indicate the cells' RF shift vectors and the black line is the vector determined by calculating the mean direction and mean amplitude of the individual vectors.

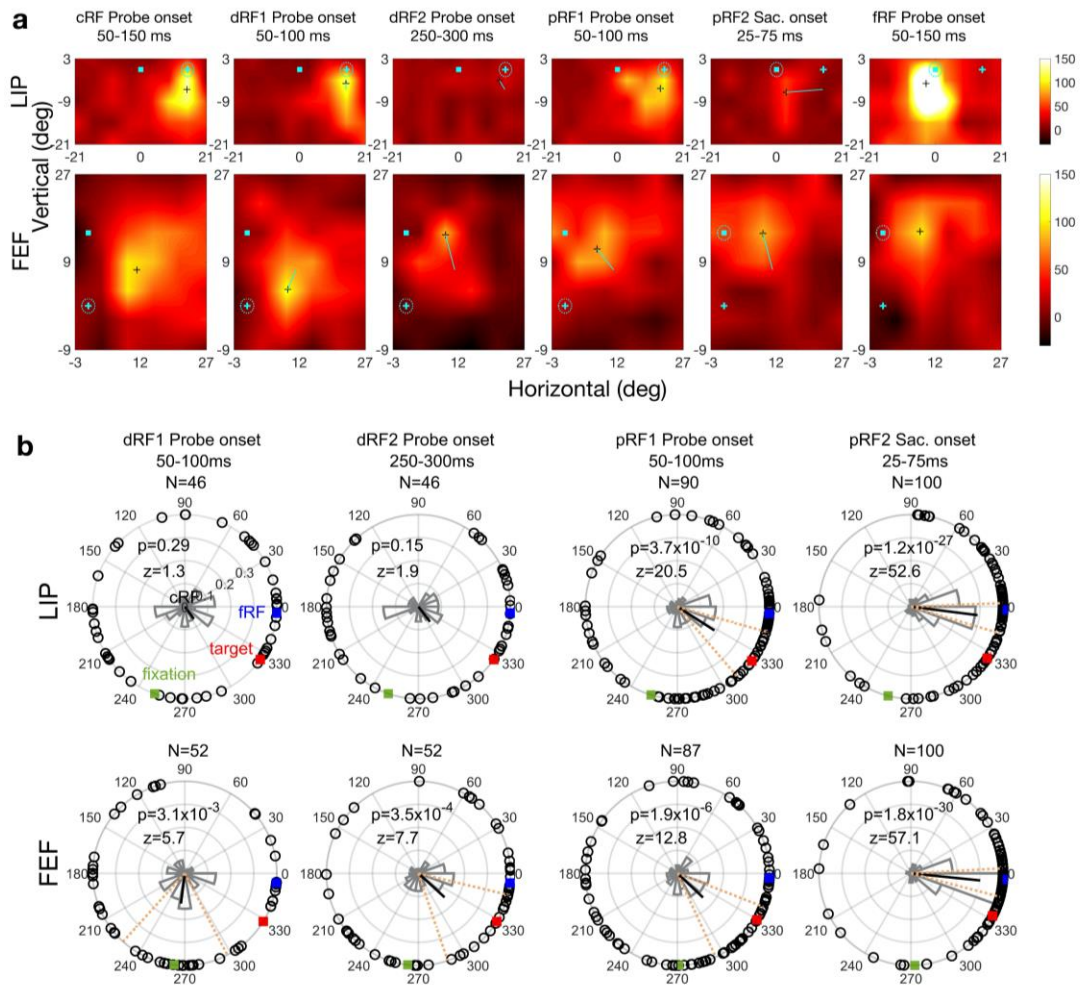


Fig. S7. RF remapping in LIP and FEF, related to Fig. 2b and StarMethods. The data analysis is identical to that for Fig. 2 in the main text but without the normalization procedure. The format is also the same as that of Fig. 2 except that in panel a, the example cells' RF heat maps are not normalized and the scales on the right indicate the firing rates (spikes/sec). The mean directions changed significantly across time in both LIP ( $p = 3.6 \times 10^{-3}$ ,  $F_{3,276} = 4.6$ ) and FEF ( $p = 9.7 \times 10^{-10}$ ,  $F_{3,287} = 16.2$ ), with Watson-Williams multi-sample test.

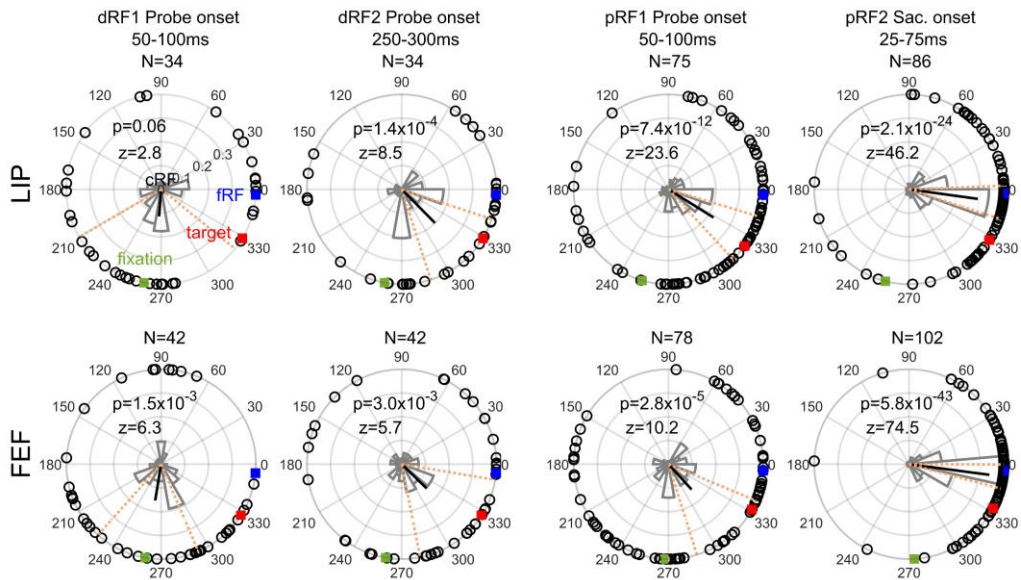


Fig. S8. RF remapping in LIP and FEF, related to Fig. 2b and StarMethods. The delay (dRF) and perrisaccadic (pRF) shift directions of LIP (top row) and FEF (bottom row) cells from different time periods (columns) are shown. The data analysis is identical to that for Fig. 2b in the main text except that in the bootstrapping step for selecting cells with significant RF shifts, we used resampling with replacement, instead of Poisson distributions. The format was identical to that of Fig. 2b in the main text. The mean directions changed significantly across time in both LIP ( $p = 2.6 \times 10^{-6}$ ,  $F_{3,225} = 10.2$ ) and FEF ( $p = 1.5 \times 10^{-10}$ ,  $F_{3,260} = 17.8$ ), with Watson-Williams multi-sample test.

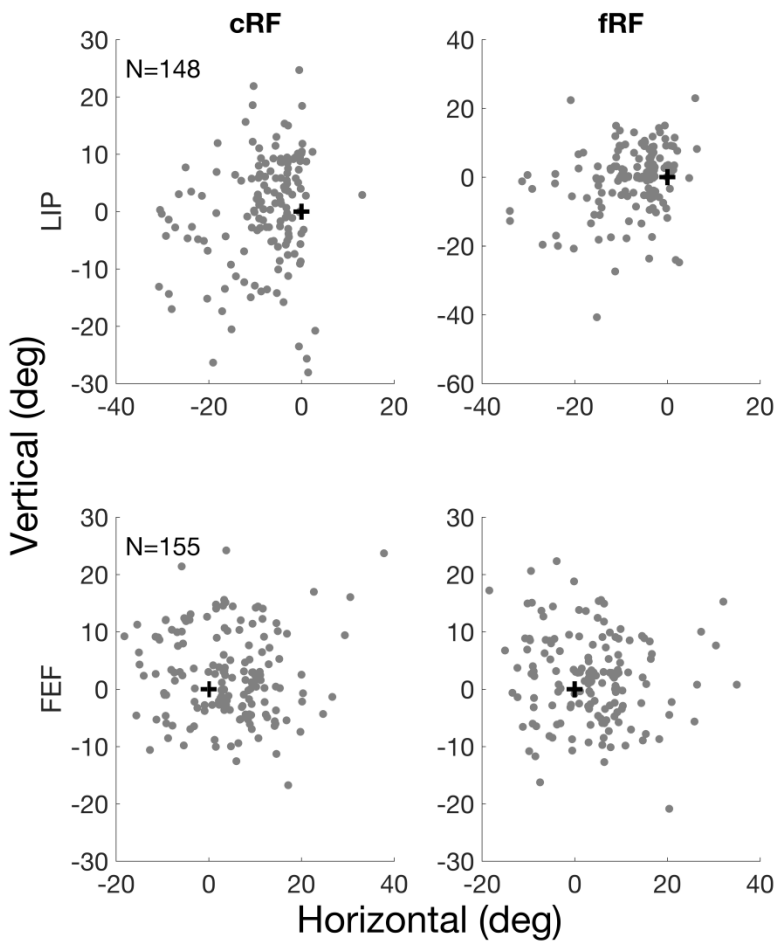


Fig. S9. Eccentricity distributions, related to Fig. 2b and StarMethods. The locations of cRF (left column) and fRF (right column) centers of LIP (top row) and FEF (bottom row) are shown. We combined the cells that passed the screening steps in the delay or perisaccadic epochs without duplication, and plotted their cRF centers relative to the initial fixation and fRF centers relative to the target. The initial fixation (for cRF) or the target (for fRF) locations were aligned at (0,0).

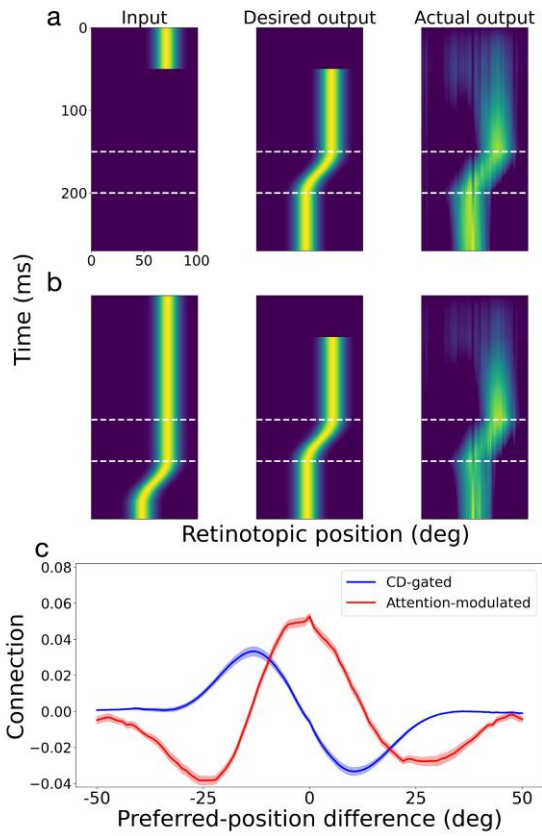


Fig. S10. Automatic generation of the required connectivity patterns in the circuit model by training a neural network, related to Fig. 7 and StarMethods. We trained the network to predictively update retinal positions of both brief (a) and persistent (b) input stimuli during saccades. The format of the figure was identical to that for Fig. 7 of the main text except that both an example of brief input (a) and an example of the persistent input (b) are shown.

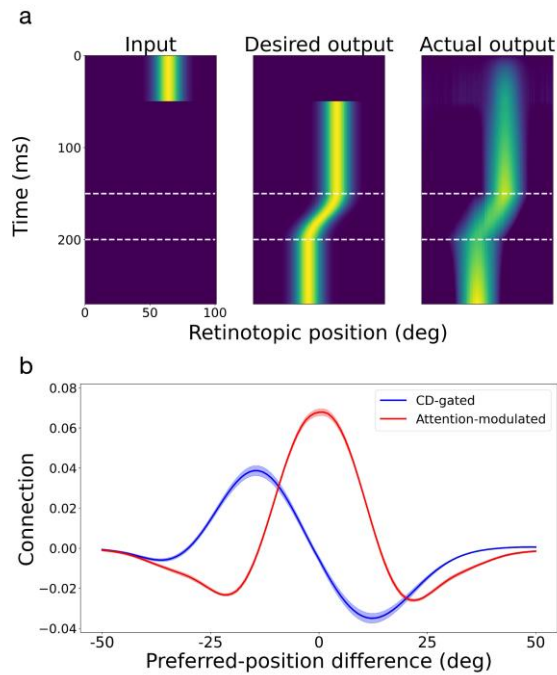


Fig. S11. Automatic generation of the required connectivity patterns in the circuit model by training a neural network, related to Fig. 7 and StarMethods. We trained the network to predictively update retinal positions of brief input stimuli during saccades without attentional modulation. We still labeled the symmetric connections (red) as attention-modulated for easy comparison with Figs. 7 and S10. The format of the figure was identical to that for Fig. 7 of the main text.

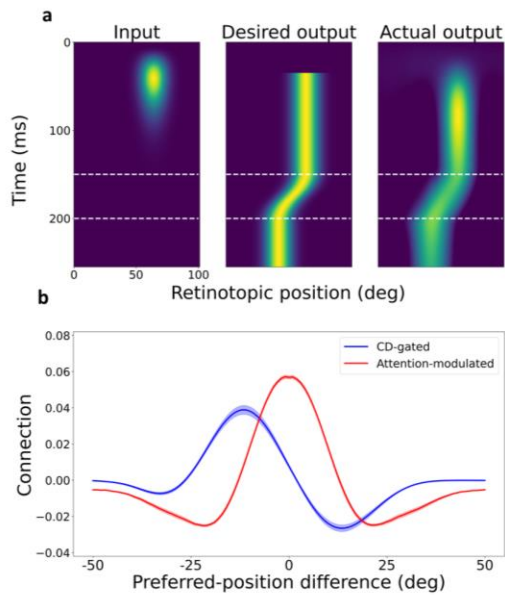


Fig. S12. Automatic generation of the required connectivity patterns in the circuit model by training a neural network, related to Fig. 7 and StarMethods. We trained the network to predictively update retinal positions of brief input stimuli during saccades without attentional modulation. It is identical to the simulation in Fig. S10 except that we used smooth functions for the temporal response of the input stimuli and the CD gating signal. The format of the figure was identical to that for Fig. S10.

Brain area	Time period	Significant visual response	Trial number $\geq 5$ within 85% contour	Completeness $\geq 80\%$ around the contour	Significant RF Shift
LIP total 391 cells	Delay (probe onset)	372	327	234	46
	Perisaccadic (probe onset)	370	305	225	91
	Perisaccadic (sac. onset)	364	298	193	104
FEF total 427 cells	Delay (probe onset)	400	367	237	57
	Perisaccadic (probe onset)	397	358	232	93
	Perisaccadic (sac. onset)	390	348	178	113

Table S1. Cell numbers, related to StarMethods. The table lists the total numbers of the recorded LIP and FEF cells and the numbers of remaining cells after each screening step. The perisaccadic results for the probe-onset and saccade-onset alignments of repeated trials are shown separately.